Journal of the European Ceramic Society **10** (1992) 393–398

Mullite Materials from a 3:2 Alumina–Silica Gel Part I: Green Processing and Porosity

C. Baudín, M. I. Osendi & S. de Aza

Instituto de Cerámica y Vidrio, CSIC, E-28500 Arganda del Rey, Madrid, Spain

(Received 11 October 1991; revised version received 13 January 1992; accepted 24 January 1992)

Abstract

The green processing parameters of a stoichiometric alumina–silica gel and their influence on the mullite bodies' final microstructures have been determined. A processing route to avoid the presence of large isolated pores, usual in mullite materials obtained from chemical precursors, has been investigated.

Es wurden die Prozeßparameter für die Grünkörperherstellung eines stöchiometrischen Aluminiumoxid–Siliziumdioxid-Gels und deren Einfluß auf das Endgefüge des gebildeten Mullit-Materials bestimmt. Des weiteren wurde eine Prozeß-Route untersucht, die die Vermeidung großer isolierter Poren ermöglicht, wie sie normalerweise in Mullit-Werkstoffen auftreten, die aus chemischen Prekursoren hergestellt werden.

Les paramètres de traitement initial d'un gel stoechiometrique d'alumine et de silice, et leur influence sur les microstructures finales de pièces de mullite ont été déterminés. Un procédé a été étudié pour éviter la présence de grands pores isolés dans des matériaux à base de mullite obtenus à partir de précurseurs chimiques.

1 Introduction

Mullite and mullite-containing composites are considered for a wide range of high performance applications such as high temperature structural components, infrared transparent windows, substrates for microelectronics, etc. To realize the full potential of mullite for technical applications, a close compositional and microstructural control of the mullite materials is required, in order to assure the optimum physical properties for each use.[1–3]

Lately, colloidal and solution techniques have revealed their capability to yield high purity mullite powders at relatively low temperatures (1000–1300°C). In addition, a number of studies have shown that densification of the mullite bodies can be enhanced by using mullite precursors in the amorphous or quasi-amorphous state.[4–6] One of the main concerns that arises when sintering compacts prepared with amorphous mullite precursors is the large weight losses that may occur at temperatures lower than 600°C.[5,6] In this case, the sintering schedule is restricted to slow heating rates in order to avoid the development of high internal pressures. Moreover, large weight losses during heating also tend to increase porosity in the compact. Consequently, mullite precursors obtained by sol–gel methods have to be pretreated at temperatures over 600°C but, in order to take advantage of the high reactivity of these powders during sintering, calcination temperatures should be lower than that of mullite formation.

Even though relatively high density mullite bodies can be obtained using sol–gel mullite precursors, two main problems arise related to the mullite bodies microstructure: the presence of large and isolated pores and the control of exaggerated grain growth.[7–10]

The processing parameters that yield high density mullite materials with controlled microstructures, small and homogeneously distributed pores, using an alumina–silica gel as starting material, will be studied in Parts I and II of this work. Part I will deal with the control of porosity by green stage processing. In Part II, the microstructural development of these mullite bodies will be studied as a function of the firing schedule.[11]

Journal of the European Ceramic Society 0955-2219/92/$5.00

2 Experimental

A colloidal type alumina–silica gel (Siral 28M, Condéa Chemie, FRG) with the chemical composition of the 3:2 stoichiometric mullite (Al_2O_3: 71·70 wt%; SiO_2: 28·04 wt%), and a total amount of impurities (Fe_2O_3, TiO_2, Na_2O, CaO, MgO) lower than 0·3 wt%, was used as the mullite precursor. A complete characterization of this powder and its thermal evolution and sintering behavior was reported previously.[6]

The as-received powders were calcined at 700, 1000 and 1300°C for 3 h and attrition milled for 2 h with mullite balls using isopropanol as the medium. Particle size distributions of the milled and unmilled powders, dispersed in isobutanol, were determined by Sedigraph (Sedigraph 5OOOET micromeritics, USA). The powders were observed by SEM. True densities of the calcined powders were determined by pycnometry, using decalin. The pore size distribution of the powder treated at 1000°C and milled was determined from the N_2 adsorptin isotherm, using the BJH approximation of the hydraulic radius.[12]

Green compacts were obtained following two routes: isostatic pressing of the powders at 200 MPa

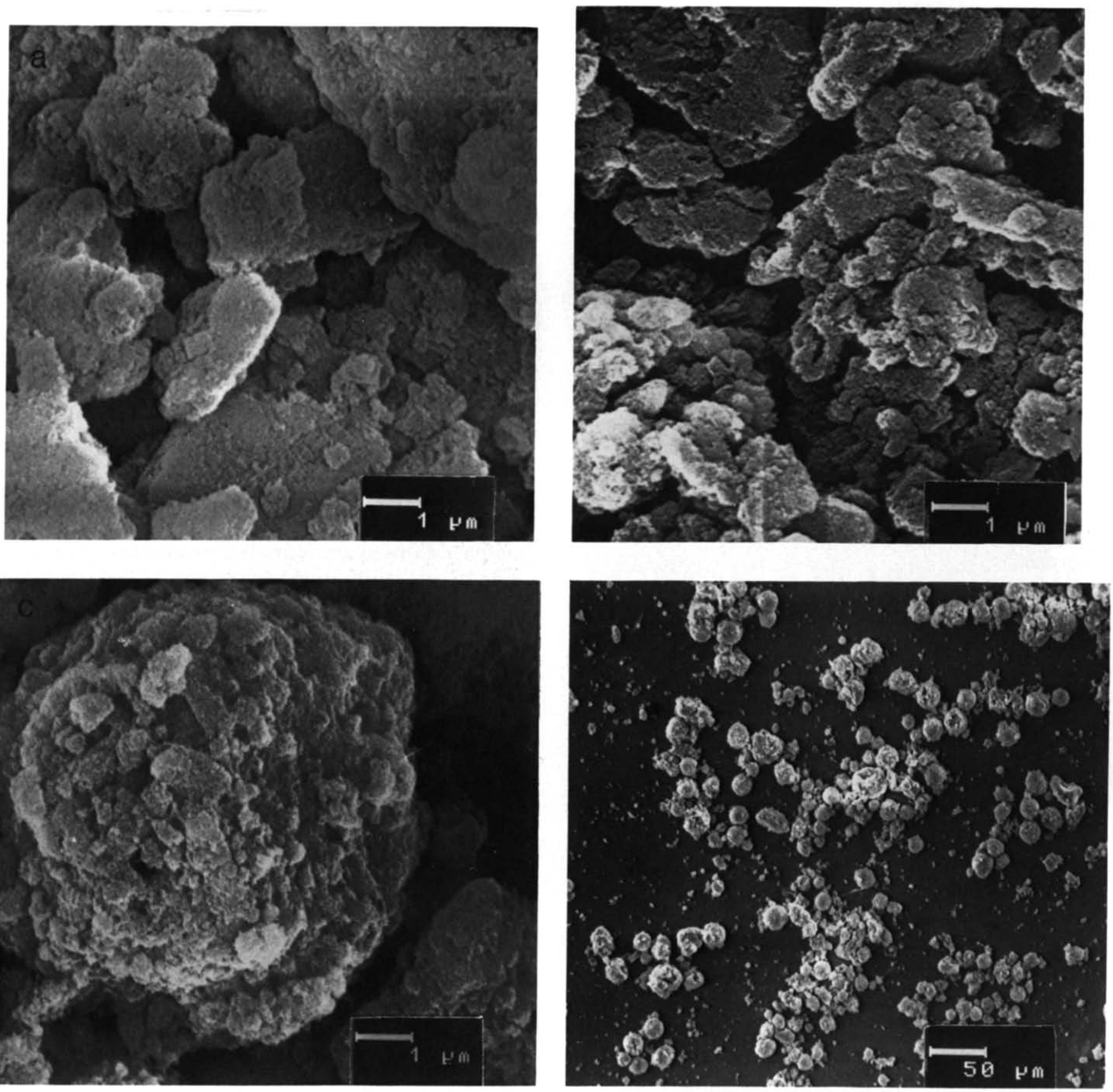

Fig. 1. Scanning electron micrographs of the powders treated at the following temperatures: (a) 700°C, (b) 1000°C, (c) and (d) 1300°C.

Table 1. Characteristics of the powders

Calcination temperature (°C)	*Density* (g/cm^3)	*Average particle diameter* (μm) *unmilled*	*Average particle diameter* (μm) *milled*
700	2·62	2·1	0·5
1 000	2·89	2·1	0·6
1 300	3·00	13·5	4·2

or uniaxial pressing at 60 MPa followed by isostatic pressing at 200 MPa. A firing schedule with isothermal steps at 1300°C–4 h and 1650°C–2 h was used for sintering. Green and fired densities were measured by the immersion method using mercury and water respectively. Reflected light optical microscopy observations were performed on polished surfaces.

3 Results

The true densities of the calcined powders are shown in Table 1; they increase with the temperature of treatment.

SEM micrographs of the thermally treated powders are shown in Fig. 1. The powders treated at low temperatures, 700 and 1000°C (Fig. 1(a) and (b)), have irregular shapes and a foaming aspect, whereas the ones treated at 1300°C (Fig. 1(c) and (d)) are round, compact, and some prismatic crystals can be differentiated on the surface.

Particle size distribution of the unmilled powders fired at 1000°C (Fig. 2), shows an average value of $\approx 2\,\mu m$ (Table 1). The average particle size of the powder treated at 1300°C is much larger, $\approx 14\,\mu m$ (Fig. 3, Table 1). Ultrasonic stirring does not lead to particle disaggregation (Fig. 3). Attrition milling of the thermally treated powders for 2 h decreases their

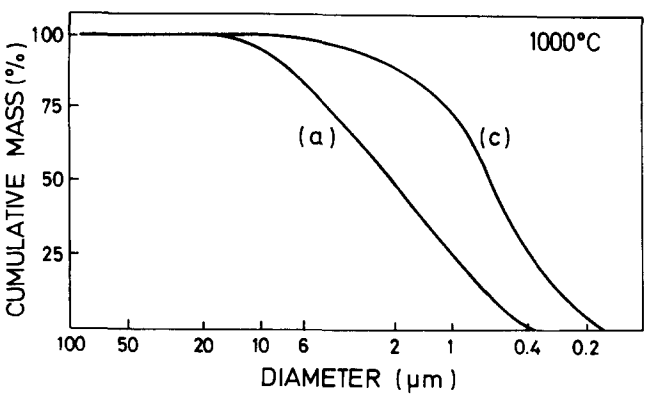

Fig. 2. Particle size distributions of the powders treated at 1000°C: (a) unmilled, (c) milled.

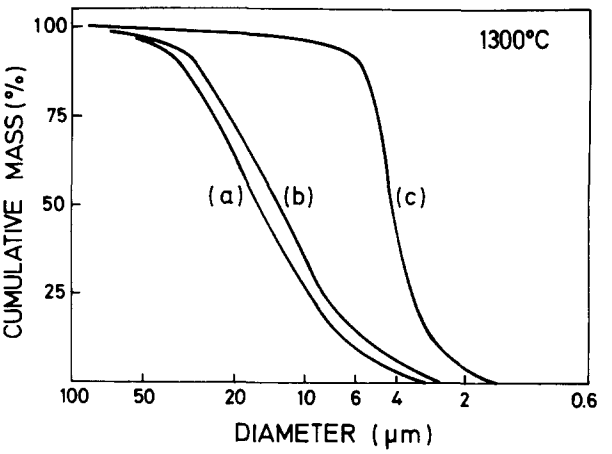

Fig. 3. Particle size distributions of the powders treated at 1300°C: (a) unmilled, (b) unmilled and ultrasonically stirred, (c) milled.

average size (Table 1) and the largest agglomerates disappear (Figs 2 and 3).

The pore size distribution of the powder treated at 1000°C and attrition milled, depicted in Fig. 4, shows that small pore sizes (<200 nm) are predominant. The BJH approximation gave the best agreement between the value of the specific surface area for pore configuration ($\approx 270\,m^2/g$) and that obtained by BET ($\approx 280\,m^2/g$). From these data, the volume of pores in the powder treated at 1000°C and milled is $0{\cdot}36\,cm^3/g$.

Table 2 shows green and fired densities of compacts made of powders treated at 1000°C, obtained in the following different ways: isostatic pressing, milling and isostatic pressing, and milling plus uniaxial followed by isostatic pressing. The largest differences are found between the fired

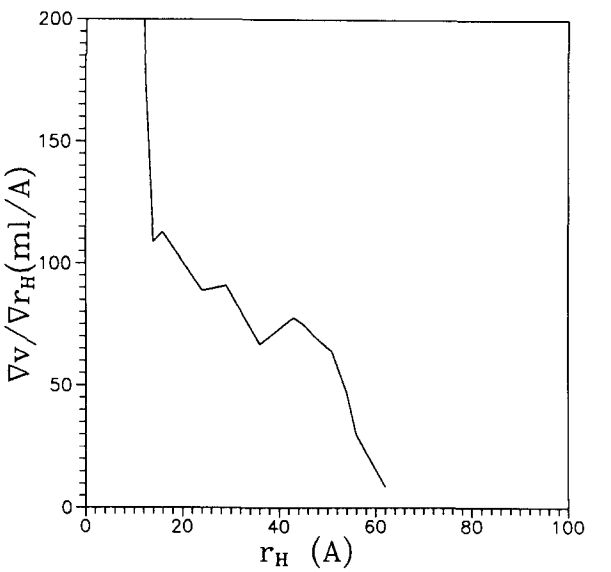

Fig. 4. Pore size distribution of the powder treated at 1000°C. Calculated from the N_2 adsorption curves using the BJH approximation.[12]

Table 2. Characteristics of the green and fired compacts

Green compact obtention	*Green density* (g/cm^3)	*Fired density* (g/cm^3)
Unmilled powders: isostatic pressing (200 MPa)	1·1	2·69
Milled powders: isostatic pressing (200 MPa)	1·2	3·14
Milled powders: uniaxial (60 MPa) + isostatic (200 MPa) pressing	1·4	3·14

densities of compacts made of milled and unmilled powders.

Low magnification micrographs of polished surfaces of the mullite bodies are shown in Fig. 5. In the samples prepared only by isostatic pressing (Fig. 5(a) and (b)) isolated large pores (≈ 100–$200\ \mu m$) are found and smaller pores are concentrated in a thin ($\approx 250\ \mu m$) outer layer. In the samples prepared following the two-step pressing process no edge effects are observed and the largest pores have been avoided ($d_{max} \approx 20\ \mu m$).

4 Discussion

True densities of the powders treated at 700 and 1000°C (Table 1) are of the same order as those reported by other authors for pseudoamorphous 3:2 mullite precursors.[13] The large increase in density between 700 and 1000°C indicates that, even though no phase changes are detected by XRD,[6] local ordering takes place in this range of temperatures.

For the powder treated at 1300°C, in which mullite is formed,[6] the density is only $\approx 94\%$ of the theoretical density for mullite (3·16 g/cm^3). This fact could be related to the closed structure of the particles that constitute this powder (Fig. 1(c)); hence trapped air inside them would mask density measurements.

The powders calcined at 1300°C are formed by

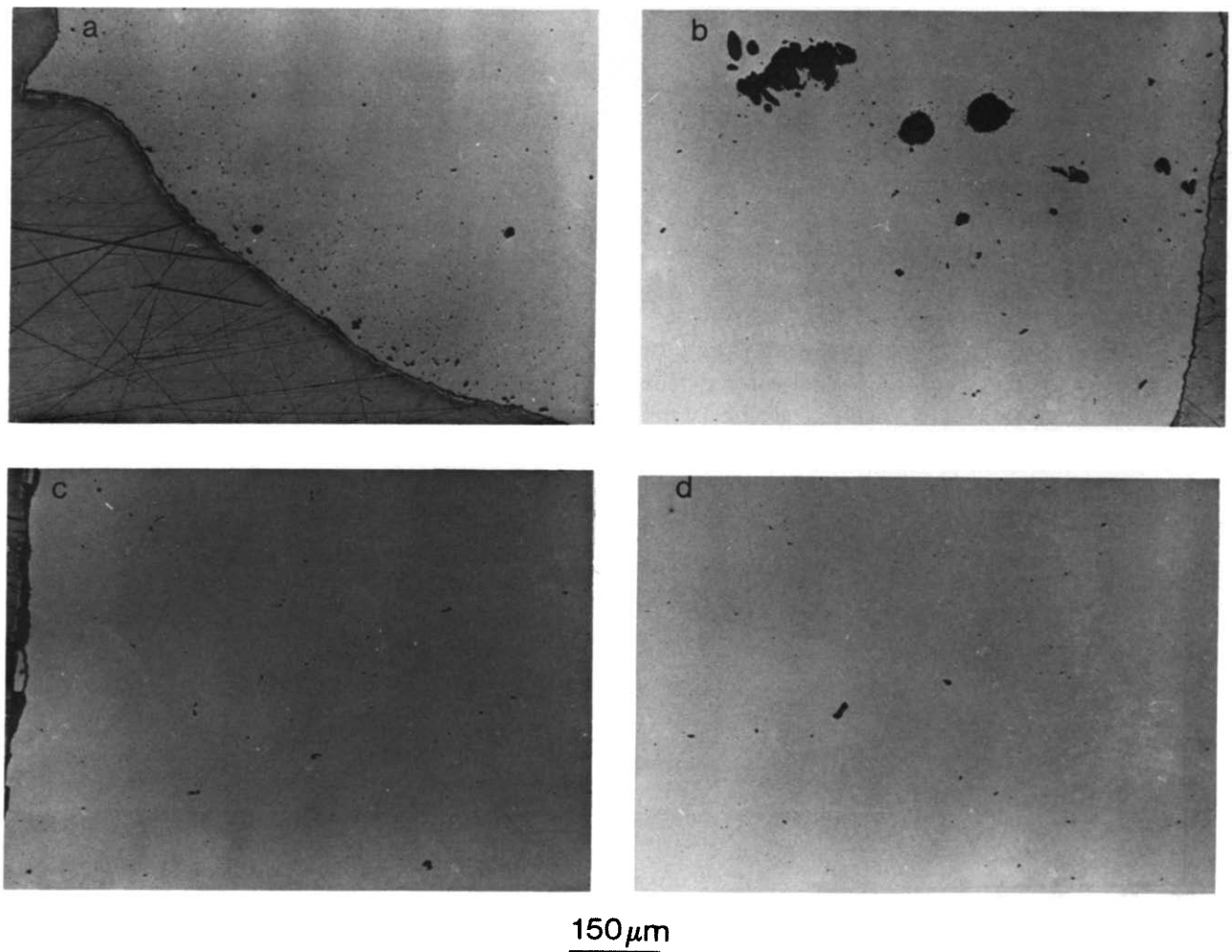

Fig. 5. Optical micrographs of mullite bodies obtained from powders treated at 1000°C: (a) and (b) green compact obtained by isostatic pressing at 200 MPa, (c) and (d) green compact obtained by uniaxial pressing at 60 MPa followed by isostatic pressing at 200 MPa.

hard agglomerates, as they cannot be disaggregated using low energy methods such as ultrasonic stirring (Fig. 3). Once mullite is nucleated, long milling periods (> 40 h for ball mill; > 10 h for attrition mill) are always required to obtain high density mullite bodies.[3,9,14–16] Although the attrition milling step does not greatly increase the green densities of the compacts, the fired densities are appreciably affected (Table 2). The diminution in aggregate size during the milling process (Table 1, Fig. 2) reduces interagglomerate pore size in the green compacts, leading to a more homogeneous sintering and, consequently, final porosity is partially eliminated.

The isolated large pores ($\approx$ 10–100 μm) observed in the fired samples (Fig. 5(a) and (b)) cannot be related to the evolution of the intraagglomerate pores that are present in the powder treated at 1000°C and milled. Firstly, this powder has small internal pores (< 500 nm, Fig. 4) and a narrow particle size distribution (Fig. 2(c)); thus pores would easily shrink or lead to homogeneously distributed porosity during sintering. Secondly, large porosity differences are found to be related to the pressing technique (Fig. 5). When the pressing stage is performed in two steps (uniaxial, 60 MPa; isostatic, 200 MPa), no edge effect and smaller pores (< 10 μm) are found (Fig. 5(c) and (d)), whereas, when a high isostatic pressure (200 MPa) is directly applied, large isolated pores ($\approx$ 100 μm) and edge effects are observed (Fig. 5(a) and (b)).

The absolute density of the powder treated at 1000°C, calculated from the true density of the powder (Table 1) and the volume of pores determined from the N_2 adsorption curve (0·36 cm^3/g), is 1·4 g/cm^3. This value coincides with the green density of the compacts obtained using the two-step pressing stage (Table 2), which means that a good compaction of the green compact is reached by this method. In this case, the porosity present in the fired compacts originates mainly from the intraagglomerate porosity; thus pores are small and uniformly distributed (Fig. 5(c) and (d)). When the green compacts are obtained by a single-step pressing stage, green densities (1·2 g/cm^3, Table 2) are lower than the calculated powder density (1·4 g/cm^3), which mean that compaction is worse than in the previously discussed case. The observed differences are related to the first pressing step which favors particle arrangement and deaeration of the compact.

As a summary, when green processing amorphous mullite precursors, a milling period as well as a pressing program with an initial smooth step have to be applied in order to counterbalance the main disadvantages of these powders: agglomerate formation during powder precalcination and the high specific surface area ($\approx$ 280 m^2/g) which leads to a high amount of trapped air and moisture.

5 Conclusions

It is possible to get large and homogeneous mullite bodies free of pores from sol–gel precursors treated at temperatures lower than that of mullite formation, by a conventional processing route.

The high specific surface areas of the powders treated at temperatures under the mullite formation temperature lead to adsorption of air and moisture during the fabrication of the green compact, which are responsible for isolated and large pore formation during sintering. This porosity can be avoided by an adequate cold pressing program.

Acknowledgements

This research was supported by CICYT (Spain), Program No. MAT88-0182.

References

1. Prochazka, S. & Klug, F. J., Infrared-transparent mullite ceramic. *J. Am. Ceram. Soc.*, **66**(12) (1983) 874–80.
2. Kanzaki, S., Kurihara, T., Iwai, S., Ohashi, M. & Tabata, H., Sintering of mullite–silica ceramics and some properties for insulating substrate material. *Yogyo Kyokai-Shi*, **95**(10) (1987) 1213–18.
3. Sacks, M. D., Lee, H.-W. & Pask, J., A review of powder methods and densification procedures for fabricating high density mullite. In *Mullite and Mullite Matrix Composites, Ceramic Transactions*, Vol. 6, ed. S. Somiya, R. F. Davis & J. A. Pask. The American Ceramic Society, OH, 1990, pp. 167–207.
4. Hirata, Y., Sakeda, K., Matshushita, Y., Shimada, K. & Ishihara, Y., Characterization and sintering behavior of alkoxide-derived aluminosilicate powders. *J. Am. Ceram. Soc.*, **72**(6) (1989) 995–1002.
5. Hirata, Y. & Shimada, K., Preparation and sinterability of fine mullite powder from mixed alkoxides. In *Mullite*, ed. S. Somiya. Uchida Rokakuho Publishing Co., Tokyo, Japan, 1985, pp. 89–122.
6. Osendi, M. I., Baudin, C., de Aza, S. & Moya, J. S., Processing and sintering of a 3:2 alumina/silica gel. *Ceram. Int.*, in press.
7. Kanzaki, S. & Tabata, H., Sintering and mechanical properties of spray pyrolyzed mullite powder. In *Mullite and Mullite Matrix Composites, Ceramic Transactions*, Vol. 6, ed. S. Somiya, R. F. Davis & J. A. Pask. The American Ceramic Society, OH, 1990, pp. 51–61.
8. Kanzaki, S., Tabata, H. & Kumazawa, T., Sintering and mechanical properties of mullite derived via spray pyrolysis. In *Mullite and Mullite Matrix Composites, Ceramic Transactions*, Vol. 6, ed. S. Somiya, R. F. Davis & J. A. Pask. The American Ceramic Society, OH, 1990, pp. 339–51.

9. Kumazawa, T., Ohta, S., Kanzaki, S. & Tabata, H., Influence of powder characteristics on microstructure and mechanical properties of mullite ceramics. In *Mullite and Mullite Matrix Composites, Ceramic Transactions*, Vol. 6, ed. S. Somiya, R. F. Davis & J. A. Pask. The American Ceramic Society, OH, 1990, pp. 401–11.
10. Mizuno, M., Shiraish, M. & Saito, H., Microstructure and bending strength of highly pure mullite ceramics. In *Mullite and Mullite Matrix Composites, Ceramic Transactions*, Vol. 6, ed. S. Somiya, R. F. Davis & J. A. Pask. The American Ceramic Society, OH, 1990, pp. 413–24.
11. Osendi, M. I., Baudín, C. & de Aza, S., Mullite materials from a 3:2 alumina–silica gel. Part II: Microstructural evolution. *J. Eur. Ceram. Soc.*, **10** (1992) 399–403.
12. Barret, E. P., Joyner, L. G. & Halenda, P. P., The determination of pore volume and area distributions in porous substances. I. Computations from nitrogen isotherms. *J. Am. Ceram. Soc.*, **73** (1951) 373–80.
13. Hori, S. & Kurita, R., Characterization and sintering of Al_2O_3–SiO_2 powders formed by chemical vapor deposition. In *Mullite and Mullite Matrix Composites, Ceramic Transactions*, Vol. 6, ed. S. Somiya, R. F. Davis & J. A. Pask. The American Ceramic Society, OH, 1990, pp. 311–22.
14. Ohnish, H., Kawanami, T., Miyazaki, K. & Hiraiwa, T., In *Ceramic Materials and Components for Engines*, ed. W. Bunk & H. Hausner. Verlag Deutsche Keramische Gesellschaft eV, Bad Honnef, 1986, pp. 633–41.
15. Kanzaki, S., Ohashi, M., Tabata, H., Kurihara, T., Iwai, S. & Wakabayashi, S., Mullite-silica ceramics for insulating-substrate material. In *Mullite and Mullite Matrix Composites, Ceramic Transactions*, Vol. 6, ed. S. Somiya, R. F. Davis & J. A. Pask. The American Ceramic Society, OH, 1990, pp. 389–99.
16. Mitachi, S., Matsuzawa, M. & Kaneko, K., Characterization of SiO_2–Al_2O_3 powders prepared from metal alkoxides. In *Mullite and Mullite Matrix Composites, Ceramic Transactions*, Vol. 6, ed. S. Somiya, R. F. Davis & J. A. Pask. The American Ceramic Society, OH, 1990, pp. 275–86.